European Journal of Medicinal Chemistry 46 (2011) 249–258

Contents lists available at ScienceDirect

European Journal of Medicinal Chemistry

journal homepage: http://www.elsevier.com/locate/ejmech

Original article

New (*RS*)-benzoxazepin-purines with antitumour activity: The chiral switch from (*RS*)-2,6-dichloro-9-[1-(*p*-nitrobenzenesulfonyl)-1,2,3,5-tetrahydro-4,1-benzoxazepin-3-yl]-9*H*-purine

Luisa C. López-Cara [a], Ana Conejo-García [a], Juan A. Marchal [b], Giuseppe Macchione [a], Olga Cruz-López [a], Houria Boulaiz [b], María A. García [b,c], Fernando Rodríguez-Serrano [b], Alberto Ramírez [b], Carlos Cativiela [d], Ana I. Jiménez [d], Juan M. García-Ruiz [e], Duane Choquesillo-Lazarte [e], Antonia Aránega [b], Joaquín M. Campos [a,*]

[a] *Departamento de Química Farmacéutica y Orgánica, Facultad de Farmacia, c/ Campus de Cartuja s/n, 18071 Granada, Spain*
[b] *Instituto de Biopatología y Medicina Regenerativa (IBIMER), Departamento de Anatomía y Embriología Humana, Facultad de Medicina, Avenida de Madrid s/n, 18071 Granada, Spain*
[c] *Unidad de Investigación, Hospital Universitario Virgen de las Nieves, Granada, Spain*
[d] *Departamento de Química Orgánica y Química Física, Facultad de Ciencias, Universidad de Zaragoza, 50009 Zaragoza, Spain*
[e] *Laboratorio de Estudios Cristalográficos, IACT, CSIC-Universidad de Granada, Av. del Conocimiento s/n, P.T. Ciencias de la Salud, 18100 Armilla, Granada, Spain*

ARTICLE INFO

Article history:
Received 14 September 2010
Received in revised form
27 October 2010
Accepted 8 November 2010
Available online 3 December 2010

Keywords:
Antitumour
Benzoxazepine
2,6-Disubstituted purine
Homochiral
MCF-7
Microwave
Seven-membered ring

ABSTRACT

Completing an SAR study, a series of (*RS*)-6-substituted-7- or 9-(1,2,3,5-tetrahydro-4,1-benzoxazepine-3-yl)-7*H* or 9*H*-purines has been prepared under microwave-assisted conditions. Their antiproliferative activities on MCF-7 and MDA-MB-231 cancerous cell lines are presented, being the majority of the IC_{50} values below 1 μM. The most active compound (*RS*)-2,6-dichloro-9-[1-(*p*-nitrobenzenesulfonyl)-1,2,3,5-tetrahydro-4,1-benzoxazepin-3-yl]-9*H*-purine (**14**) presents an IC_{50} of 0.166 μM against the human cancerous cell line MDA-MB-231. Compound **14** was the most selective against the human breast adenocarcinoma MCF-7 and MDA-MB-231 cancer cell lines (Therapeutic Indexes, TIs = 5.1 and 11.0, respectively) in relation to the normal one MCF-10A. (*RS*)-**14** was resolved into its enantiomers. Both enantiomers are equally potent, but more potent than the corresponding racemic mixture. (*R*)-**14** induces apoptosis against MCF-7 up to 52.50% of cell population after 48 h, being more potent than the clinical-used drug paclitaxel (43%). (*RS*)-**14** induces no acute toxicity in mice after two weeks of treatment.

1. Introduction

With more than 10 million new cases each year cancer is at present one of the most devastating diseases worldwide with an immense affliction burden not only for affected individuals, their relatives and friends but also representing heavy challenges to health care systems [1]. In the year 2000, cancer was responsible for 12% of the nearly 56 million deaths worldwide and in many countries this percentage is even higher with more than a quarter of deaths attributable to cancer. Moreover, it is expected that cancer rates can further increase by 50% to 15 million new cases in the year 2020, mainly due to steadily ageing populations in both developed and developing countries [2].

In recent years, many studies have shown an association between cell-cycle regulation and cancer inasmuch as the cell-cycle inhibitors are being considered as a weapon for the management of cancer [3]. Ultimately a great level of interest has arisen in the G_0/G_1 phase regulatory molecules such as cyclin D1, CdkIs, and p53 as potential therapeutic targets in diseases where control of inappropriate cellular proliferation would be a therapeutic benefit [4].

Apoptosis is an essential physiological process throughout the life of multi-cellular organisms important in the development and in the maintenance of tissue homeostasis. Apoptosis is involved in controlling the cell number and proliferation during embryogenesis, deletion of activated lymphocytes at the end of the immune response, elimination of self-reactive lymphocytes, in controlled destruction of damaged, aged, infected, transformed, and other harmful cells [5,6]. Zivny et al. have recently reviewed the apoptotic pathways, molecules involved in the cross-talk between individual apoptosis pathways,

* Corresponding author. Tel.: +34 958 243848; fax: +34 958 243845.
E-mail address: jmcampos@ugr.es (J.M. Campos).

0223-5234/$ – see front matter © 2010 Elsevier Masson SAS. All rights reserved.
doi:10.1016/j.ejmech.2010.11.011

apoptosis regulation as well as mechanisms of action of conventional anticancer drugs and new promising agents, which trigger directly or indirectly apoptosis of hematologic cancer cells [7].

We have reported the synthesis and anticancer activities of compounds **1**–**3**, **5**–**6** [8] and *trans*-**7** [9] (Chart 1). In all the cases, the linkage between the 5-fluorouracil (5-FU) moiety and the seven-membered ring was carried out through its $N-1$ atom.

The structural nature of **6** implies that this compound cannot be considered as a 5-FU prodrug and we suspected that neither would the remaining compounds (**1**–**3**, **5**–**7**) be 5-FU prodrugs [10]. The effects of the uracil benzo-fused seven-membered *O*,*N*-acetal **4** were investigated in the MCF-7 human breast cancer cell line. The expression of cell-cycle-related proteins (cyclin D1, and p53) was also explored to investigate the potential mechanisms of the G_0/G_1 arrest activity of **4** [10]. In addition, the expression levels of CDKIs, such as p21Waf1/Cip1 and p27Kip1, were examined in MCF-7 cells [10].

We have reported that compounds **8** and **9**, with a thymine linked to a seven-membered ring (Chart 2) exhibited *in vitro* antiproliferative activities (12.74 ± 4.79 and 30.05 ± 0.71 μM, respectively) against the MCF-7 cell line [11].

Moreover, the uracil *O*,*N*-acetals **10**–**13** (Chart 3) derived from the tetrahydrobenzoxazepine moiety, whose syntheses were reported [12], show *in vitro* antiproliferative activities against the MCF-7 human breast cancer cell line in the micromolar range [13].

Taken together, the antiproliferative activities of the naturally occurring pyrimidine compounds **8**–**13** are an outstanding fact that has not been previously reported in bibliography. Therefore these compounds may serve as prototypes for the development of even more potent structures, endowed with a new mechanism of action. Once the alkylated pyrimidine derivatives had been studied, the shift was made to the more lipophilic purine ones [14]. Herein we will report the synthesis and antiproliferative activities of purine derivatives **14**–**24** (Chart 4) against the cancerous MCF-7 and MDA-MB-231 human breast cancer cell lines and the corresponding normal one (MCF-10A) to define the *in vitro* TI as a measure of the selectivity. From a structural point of view, the compounds studied herein differ from others previously reported [13] by the addition of an extra halogen or PhS- groups on the purine ring. Finally the most active racemic compound was resolved and the antiproliferative activity of its enantiomers was measured.

Modern drug discovery relies on high speed organic synthesis. Microwave-assisted organic synthesis [15–21] is proving to be instrumental for the rapid synthesis of compounds with new and improved biological activities [22,23]. We previously investigated the Vorbrüggen condensation in microwave-assisted organic synthesis [24]. Microwave advantage is chiefly the quick access to the target molecules as well as the better yield obtained in the only isomer formed making the purification processes much easier.

2. Results and discussion

2.1. Chemistry

2.1.1. Synthesis of derivatives

Preparation of the *O*,*N*-acetals **14**–**17** was achieved by the microwave-assisted Vorbrüggen one-pot condensation of the cyclic acetals **25** and **26** [25] and the commercially available purine bases 6-chloro-, 6-bromo- and 2,6-dichloro-purines, using chlorotrimethylsilane (TMSCl), 1,1,1,3,3,3-hexamethyldisilazane (HMDS) and tin(IV) chloride as the Lewis acid in anhydrous acetonitrile. The reaction mixture was microwave-irradiated at a temperature of 140 °C or 160 °C for 5 min (Scheme 1). Compounds **27** and **28** were isolated from the reactions and the acyclic *O*,*N*-acetal **23** was also obtained in the synthesis of **14**. Traces of the *N*-7′ regioisomer **24** were detected in the synthesis of **15**. The following modifications were carried out on **15**: a) selective nucleophilic substitution of the chorine atom at position 6 of the purine ring using NaI and trifluoroacetic acid (TFA) to yield **18**; b) reduction of the nitro group with $SnCl_2$ to give rise to **19** and **20**; and c) the treatment with the PhSH to produce **21** and **22** (see Experimental Part for details).

2.1.2. Other products in the reaction between acetals *25* and *26* and purines

Compounds **27** and **28** were obtained along with the cyclic and acyclic *O*,*N*-acetals in the reaction of purines with **25** and **26**, respectively. Their importance lies in the information that they provide on the mechanism of the reaction with purines as none of these olefins have

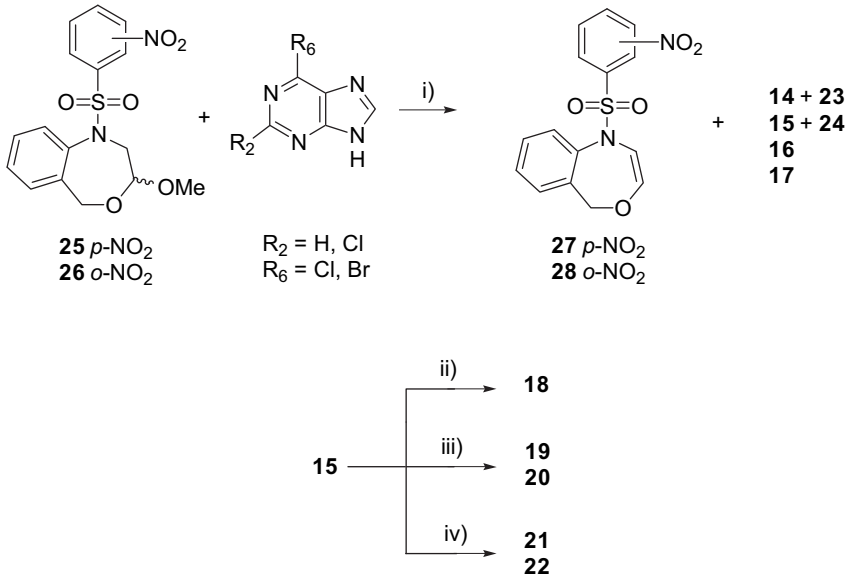

Scheme 1. Reagents and conditions: i) purine, TMSCl, HMDS, $SnCl_4$ (1 M solution in CH_2Cl_2), 140 or 160 °C, microwave, 5 min; ii) NaI, TFA, butanone, −15 °C, 6 h; iii) $SnCl_2 \cdot 2H_2O$, EtOH, reflux, 2 h; iv) PhSH, K_2CO_3, DMF, rt, 4 h.

been isolated in the corresponding reactions with uracil or 5-FU [12]. Although it could have been thought that the formation of the seven-membered sulfonenamides **27** and **28** was simply due to an elimination of methanol from the cyclic *O,O*-acetals **25** and **26**, our previous results reported on the acyclic *O,N*-acetals 6-chloro-7-{2-[*N*-(2-hydroxymethylphenyl)-2- or 4-nitrobenzenesulfonamide]-1-methoxyethyl}-7*H*-purines clearly support a more complicated reaction mechanism [26].

Compounds **27** and **28** could have been originated in a process which shared the reaction mechanism with the *N*-7″ → *N*-9″ transformation, *via* elimination of the purine ring after its activation as a leaving group by the coordination of the Lewis acid to one of its electron-rich positions. This elimination would be easier for the highest energy *N*-7″ regioisomers than for the more stable *N*-9″ ones. The formation of the cyclic olefin would be justified by the resonance of the final electronic system.

According to an elimination mechanism, loss of the purine ring would lead to the oxocarbenium ions **29** and **30**, which could either attack nucleophile positions of the purine giving rise to the formation of the *N*-9″ *O,N*-acetals (**14**–**17**), or eliminate one β proton in relation to the O^+ atom, with formation of a double bond to give **27** and **28** (Scheme 2). The progress of the cationic intermediate in one way or another would depend on the speed of each process.

2.1.3. Homochiral drugs

The issue of drug chirality is now a major theme in the design and development of new drugs, underpinned by a new understanding of the role of molecular recognition in many pharmacologically relevant events. In general, three methods are utilized for the production of a chiral drug: the chiral pool, separation of racemates, and asymmetric synthesis. Although the use of chiral drugs predates modern medicine, only since the 1980's has there been a significant increase in the development of chiral pharmaceutical drugs. An important commercial reason is that as patents on racemic drugs expire, pharmaceutical companies have the opportunity to extend patent coverage through development of the chiral switch enantiomers with desired bioactivity [27].

2.1.4. Resolution of (RS)-14 into its two enantiomers

(*RS*)-9-[1-(*p*-Nitrobenzenesulfonyl)-1,2,3,5-tetrahydro-4,1-benzoxazepin-3-yl]-2,6-dichloro-9*H*-purine (**14**) is resolved into its two enantiomers: [(*R*)-**14**: $[\alpha]^{25}_{D} = -43.6$ (c = 0.22, THF), and (*S*)-**14**: $[\alpha]^{25}_{D} = +41.0$ (c = 0.23, THF)] using a semipreparative column CHIRALPAK® and a mixture of hexane/*t*-BuOMe/*i*PrOH as eluant [28]. The details for the X-ray data for enantiomer (*S*)-**14** are shown in the Supporting Information Section.

2.2. Biological activities

Table 1 shows the antiproliferative activity (IC_{50} values) for **14**–**24** and **27**, **28**. All the compounds were first assayed as antiproliferative agents against the human breast adenocarcinoma cell line MCF-7 (p53 wild-type and ras mutated). The seven most active compounds (**14, 15, 18**–**20**, and **23**–**24**) were selected to be further assayed on the human breast cancer cell line MDA-MB-231, which has high levels of mutant p53, the most commonly mutated gene in human cancer. Additionally, we used a non-cancerous human mammary epithelial cell line (MCF-10A), in order to study the therapeutic index against breast cancer.

It must be pointed out that from the twenty IC_{50} values against the two cancerous cell lines, the majority of the IC_{50} values were below 1 μM. As shown in Table 1, all compounds were more active as antiproliferative agents against MDA-MB-231 than against the MCF-7 human breast cancer cell line, except for the acyclic derivative **23**, whose antiproliferative effect remains the same in both cancer cell lines. The $IC_{50} = 0.166$ μM for compound **14** against the

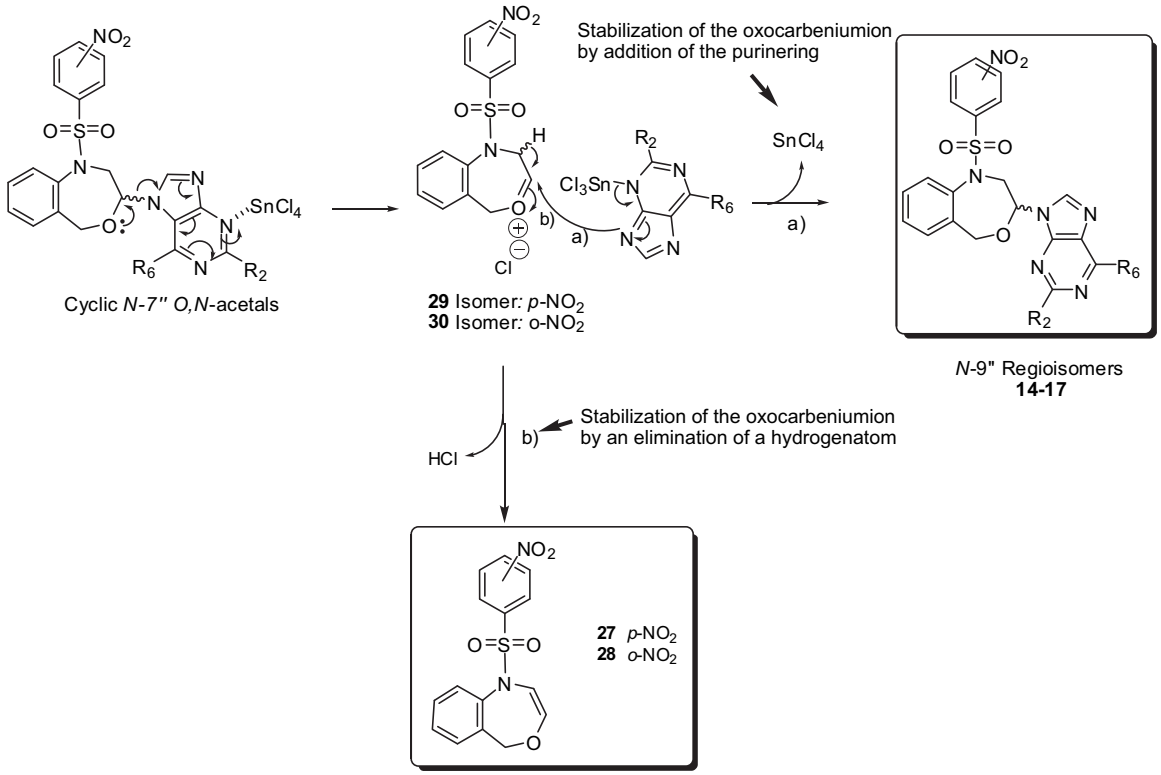

Scheme 2. Mechanism proposed for the formation of 1,5-dihydro-4,1-benzoxazepines **27** and **28** from cyclic *N*-7″ *O,N*-acetals.

Table 1
Antiproliferative activities[a] for compounds **14**–**24** against the cancerous cell lines MCF-7 and MDA-MB-231, and the non-cancerous cell line MCF-10A.

Compound	IC_{50} MCF-7 (μM)	IC_{50} MDA-MB-231 (μM)	IC_{50} MCF-10A (μM)
14	0.355 ± 0.011	0.166 ± 0.063	1.825 ± 0.503
15	0.383 ± 0.027	0.280 ± 0.006	1.530 ± 0.198
16	1.226 ± 0.348	N.D.[b]	N.D.[b]
17	3.618 ± 0.273	N.D.[b]	N.D.[b]
18	0.610 ± 0.043	0.256 ± 0.002	0.351 ± 0.020
19	0.820 ± 0.050	0.467 ± 0.017	1.520 ± 0.498
20	1.530 ± 0.040	0.487 ± 0.006	1.233 ± 0.217
21	9.710 ± 0.380	N.D.[b]	N.D.[b]
22	13.85 ± 1.790	N.D.[b]	N.D.[b]
23	0.355 ± 0.122	0.409 ± 0.074	1.863 ± 0.050
24	0.990 ± 0.090	0.318 ± 0.066	1.265 ± 0.163
5-FU[c]	4.32 ± 0.020	N.D.[b]	N.D.[b]

[a] All experiments were conducted in duplicate and gave similar results. The data are means ± SEM of three independent determinations. The treatment time was 48 h.
[b] N.D. = Not determined.
[c] Taken from Ref. [14].

human cancerous cell line MDA-MB-231 stands out over the rest of the values (Fig. 1).

A comparison between the cancerous cell lines (MCF-7 and MDA-MB-231) and the corresponding normal one (MCF-10A) was established in an intent to define the *in vitro* therapeutic index as a measure of the selectivity. The *in vitro* therapeutic index (TI) of a drug is defined as the ratio of the toxic dose to the therapeutic dose (*In vitro* TI = IC_{50} non-tumour cell line/IC_{50} tumour cell line) [29]. TI was better for compounds **14**, **15** and **23** against both cancer cell lines with values up to 11.0, 5.50 and 4.55, respectively against MDA-MB-231 cell line. 2,6-Dichloro derivatives **14** and **23** were the most selective compounds against the human breast adenocarcinoma MCF-7 cancer cell line (TIs = 5.1 and 5.2, respectively) in relation to the normal one. The iodine derivative **18** showed the most toxic effect against the non-tumour MCF-10A human mammary epithelial cell line (Table 2, Fig. 1).

2.2.1. *In vitro cytotoxic activities*

When the homochiral forms were analyzed we found differences in the IC_{50} values between (*S*)-**14** and (*R*)-**14** enantiomers, although no differences in activity were found between the two enantiomers against the MDA-MB-231 cell line. However both enantiomers present higher antiproliferative activity than the

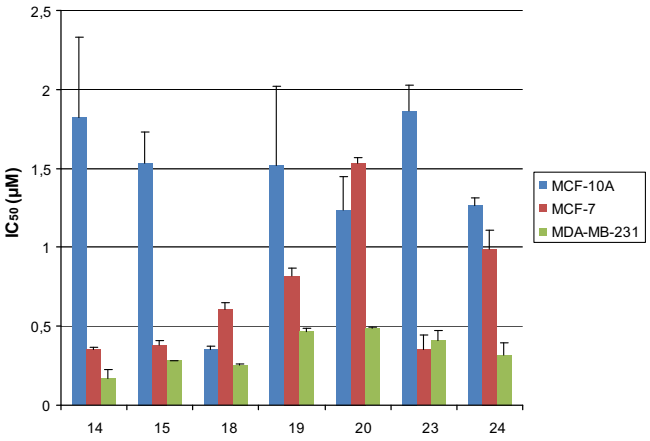

Fig. 1. Comparison between antiproliferative activities for the most representative compounds against the cancerous cell lines MCF-7 and MDA-MB-231, and the non-cancerous cell line MCF-10A.

Table 2
Therapeutic indexes for the most representative compounds.

Compound	Therapeutic index (TI)	
	MCF-7	MDA-MB-231
14	5.14	11.0
15	4.00	5.50
18	0.57	1.37
19	1.85	3.25
20	0.80	2.53
23	5.25	4.55
24	1.27	4.00

racemic compound showing the greatest differences against MCF-7 cells. (*S*)-**14** shows higher antitumour activity, up to twice that of (*R*)-**14** in the MCF-7 cell line. Studies with other compounds showed similar results with more potency in cytotoxicity in an enantiomer in comparison with the racemate. This enantioselective cytotoxicity indicates that the enantiomers of some chiral drugs may differ both quantitatively and qualitatively in their biological activity [30,31]. Moreover, enantiomers can posses minimal *in vitro* but a dramatic *in vivo* chiral dependency in their antitumour activities [32,33] (Table 3).

2.2.2. *Selection of compounds to study the cell cycle*

Once the antitumour activity of compounds was determined against the different breast cell lines, we carried out a selection between those that showed a great cytotoxic effect against MCF-7, including (*R*)-**14** and (*S*)-**14**, in order to determine their influence on the several cell-cycle phases. In this study we have included drugs used in clinic against breast cancer, such 5-FU and paclitaxel, with a known mechanism of action at the level of cell cycle.

2.2.3. *Cell-cycle analysis*

In order to analyze if the antitumour effects of the drugs involve changes in cell-cycle distribution, the non-tumour cell line MCF-10A and the breast cancer cell lines MCF-7 and MDA-MB-231 were treated with the compounds during 48 h and then analyzed by flow cytometry (Supporting Information Tables 1–3). The non-accumulation in a specific phase was detected during treatment with the drugs in most of the cell lines analyzed in comparison with control-DMSO-treated cells. Only the (*R*)-**14** enantiomer was able to induce in MDA-MB-231 cells an accumulation in both G_0/G_1 and G_2/M phases with the consequently significant decreased in the S phase. Also an accumulation in the phase G_2/M was detected in MCF-7-**18** treated cells. Treatment with 5-FU and paclitaxel, as have been described previously [34], induced accumulation in the S or G_2/M phases depending on the cell line analyzed. Similar data were obtained when cell lines were treated for 24 h with 0.5 mM mimosine to synchronize the cells in the G_1/S phase (data not shown). These results indicate that compounds inhibited all phases of the cell cycle, probably through the inhibition of protein synthesis as it has been proved with other antitumour drugs [35].

Table 3
Antiproliferative activities of (*RS*)-**14** and its enantiomers against the cancerous cell lines MCF-7 and MDA-MB-231.

Compound	MCF-7 (μM)	MDA-MB-231 (μM)
14	0.355 ± 0.011	0.166 ± 0.063
(*R*)-**14**	0.19 ± 0.001	0.11 ± 0.001
(*S*)-**14**	0.10 ± 0.001	0.11 ± 0.001

All experiments were conducted in duplicate and gave similar results. The data are means ± SEM of three independent determinations.

2.2.4. Apoptosis assay

Finally, to determine if the observed growth inhibition was due to apoptosis, both flow cytometry and confocal microscopy studies were carried out. The cells were treated with the IC_{50} values of compounds and stained using Annexin V and propidium iodide (PI) at 24 and 48 h post-drug treatment. Apoptosis assays were accomplished in the MCF-7 human breast cancer cell line, where the demonstration of programmed cell death by known apoptosis-inducing agents has proven difficult and only few cytotoxic agents act preferentially through an apoptotic mechanism in human breast cancer cells [36,37]. Paclitaxel (TAXOL®) induced programmed cell death of up to 43% of the cell population. Simultaneous staining with annexin V-FITC and the PI non-vital dye made it possible to distinguish between early apoptosis (stained positive for annexin V-FITC and negative for PI), and late apoptosis or cell death (stained positive for both annexin V-FITC and PI). In MCF-7 control-DMSO cultures neither early nor late apoptosis were detected after 24 h or 48 h. Similarly, compounds did not induce apoptosis after 24 h of treatment (Supporting Information, Table 4). In contrast, MCF-7 cells treated during 48 h with the novel compounds showed a significant increase of early apoptotic cells in relation to the control culture with percentages varying from 13.93% in cells treated with **24** to 43.30% and 41.99% after treatment with **23** and (*R*)-**14**, respectively. The percentage of late apoptotic cells also increased in MCF-7 cells treated with the drugs in comparison with control-DMSO-treated cells (Table 5 Supporting Information). It should be noted that levels of early apoptosis induced by (*R*)-**14** were almost double in comparison with the corresponding racemic compound **14,** which may explain the enantioselective antiproliferative activity shown by this enantiomer. These high apoptotic percentages shown by (*R*)-**14** are consistent with the G_1 and G_2/M arrest since cells exposed to specific agents typically enter apoptosis from a given phase of the cell cycle [10,36,38,39]. Differences in cytotoxicity, cell-cycle analysis or apoptotic levels between (*R*)-**14** and (*S*)-**14** suggest distinct signalling pathways as has been shown with other antitumour enantiomers [40]. Moreover, the amount of cells undergoing apoptosis in response to the compounds may likely have been higher than these values, due to the fact that only adherent cells were stained and counted. Representative results for the MCF-7 cells at 48 h of treatments are shown in Fig. 2A.

The effects of compounds on the pattern of cell death were also confirmed by confocal microscopy after staining with FITC-conjugated annexin V and the nuclear non-vital stain PI. MCF-7 cells treated with compounds showed several staining patterns (Fig. 2B). Some cells displayed an intense FITC staining located at the plasma membrane and a nucleus with intensely PI-labeled marginated chromatin, suggesting that they were in the course of apoptosis. Other cells showed a peculiar staining pattern, because they exhibited nuclei with the same features observed in true apoptotic cells and, at the same time, cytoplasms homogeneously stained for annexin V. In fact, the FITC staining was located not only at the cell surface, but also within the cytoplasm (Fig. 2B). Therefore, these cells were considered as aponecrotic cells as previously has been established [41]. In addition, patches of localised partially condensed chromatin were found in other cells abutted along the inner part of the nuclear membrane (Fig. 2B). In the control cultures, most of the cells turned out to be negative for both staining except for some dying cells with the staining features of apoptosis (data not shown). The present data support the effect of the compounds in some of the series of steps of the apoptotic process where a wide range of intermediate morphological and biochemical types of cell death occur [38,42].

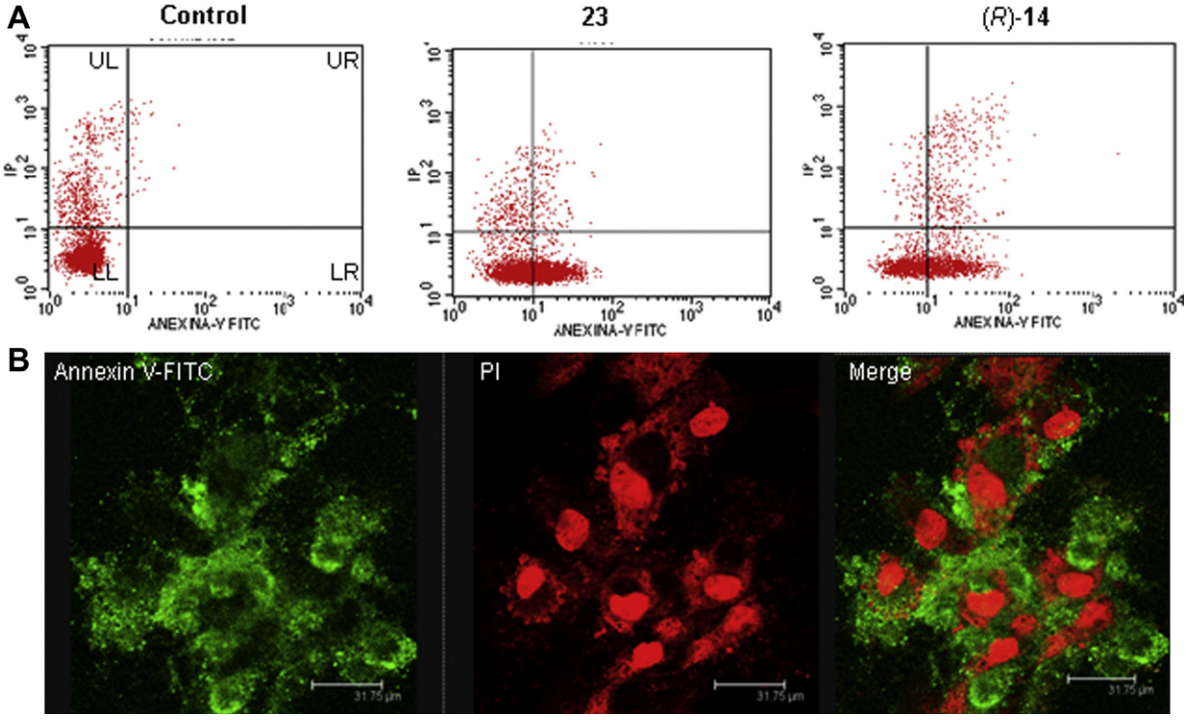

Fig. 2. Apoptosis induction in the MCF-7 human breast cancer cell line after treatment for 48 h with the compounds. (A) Representative panels of cytometry analysis for control cells treated with 0.5% DMSO alone, **23** and (*R*)-**14**. In each panel, lower left quadrant (LL) shows viable cells which are negative for both annexin V-FITC and PI, lower right (LR) shows annexin V positive cells which are in the early stage of apoptosis, upper left (UL) shows only PI positive cells which are dead, and upper right (UR) shows both annexin V and PI positive, which are in the stage of late apoptosis. (B) Confocal microscopy analysis using simultaneous staining with annexin V-FITC (green) and PI (red) in MCF-7 after treatment with **23**. (For interpretation of the references to colour in this figure legend, the reader is referred to the web version of this article).

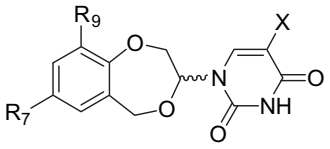

1 $R_7 = R_9 = H$, X = F
2 R_7 = OMe; R_9 = H; X = F
3 R_7 = H; R_9 = OMe; X = F
4 $R_7 = R_9 = H$; X = H

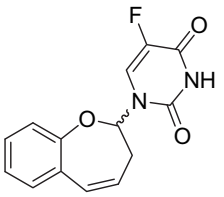

5

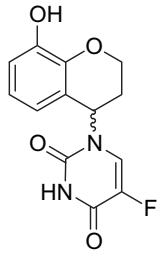

6

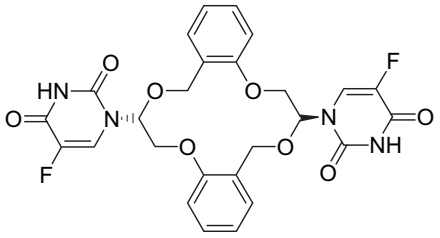

7

Chart 1.

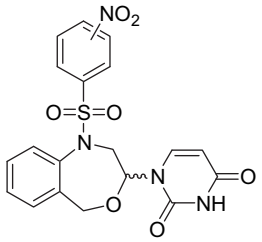

10 *ortho* isomer; IC_{50}: 45.17± 0.48 μM
12 *para* isomer; IC_{50}: 39.78±2.60 μM

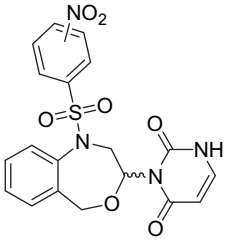

11 *ortho* isomer; IC_{50}: 50.90±3.87 μM
13 *para* isomer; IC_{50}: 44.28± 4.65 μM

Chart 3.

2.2.5. In vivo toxicity

Toxicity was determined selecting (*RS*)-**14,** which was the most *in vitro* cytotoxic compound against MCF-7 cells. We examined the acute-toxicity profile of (*RS*)-**14** in BALB/c mice when it was administered in a single i.p. bolus injection ($n = 25$) at dose levels of 50, 75, 100, 150 and 200 mg/kg or *via* gavage ($n = 25$) in a single p.o. bolus at dose levels of 0.05, 0.5, 5 and 50 mg/kg. (*RS*)-**14** was nontoxic to BALB/c mice even at the highest i.p. bolus dose of 200 mg/kg and p.o. bolus dose of 50 mg/kg after 2 weeks. Control mice ($n = 10$; 5 mice for the i.p. group and 5 mice for the p.o. group) were treated with vehicle alone. All 50 (*RS*)-**14**-treated mice remained healthy and gained weight throughout the 15-day observation period, with no evidence of morbidity.

3. Conclusion

The anticarcinogenic potency of the target molecules is reported against one non-tumour cell line and two cancerous ones. The most active compound (**14**) presents an IC_{50} of 166 nM, being the most potent structure so far reported. These results provide promising information for further development of potent antiproliferative agents. Compound **14** induces no acute toxicity in mice after 2 weeks of treatment. Compound **14** and its enantiomers associated with the inhibition of cancer cell proliferation caused in MCF-7 and MDA-MB-231 cells would make them very attractive agents, opening a new strategy in cancer chemotherapy using similar compounds endowed with potent antitumour activities with future clinical application in breast cancer. At present, studies are being carried out to determine the mechanism of action at the molecular level of the most active compounds.

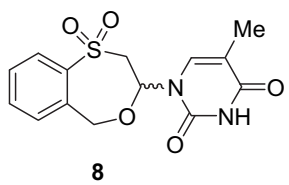

8

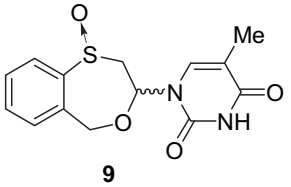

9

Chart 2.

4. Experimental protocols

4.1. Chemistry

Melting points were taken in open capillaries on an Electrothermal melting point apparatus and are uncorrected. Nuclear magnetic resonance spectra were recorded on a 400 MHz ^1H and 100 MHz ^{13}C NMR Varian NMR-System-TM 400 or 300 MHz ^1H and 75 MHz ^{13}C NMR Varian Inova-TM spectrometers at ambient temperature. Chemical shifts (δ) are quoted in parts per million (ppm) and are referenced to the residual solvent peak. Signals are designated as follows: s, singlet; d, doublet; dd, doublet of doublets; ddd, double doublet of doublets; dt, doublet of triplets; t, triplet; pt, pseudotriplet; m, multiplet. High-resolution liquid secondary ion mass spectra (HR LSIMS) were carried out on a VG AutoSpec Q high-resolution mass spectrometer (Fisons Instruments). Small scale microwave-assisted synthesis was carried out in an Initiator 2.0 single-mode microwave instrument producing controlled irradiation at 2.450 GHz (Biotage AB, Uppsala). Reaction time refers to hold time at 160 °C or 140 °C, not to total irradiation time. The temperature was measured with an IR sensor on the outside of the reaction vessel. Anhydrous acetonitrile was purchased from VWR International Eurolab. 6-Chloropurine, 6-bromopurine and 2,6-dichloropurine were purchased from Aldrich. Analyses indicated by the symbols of the elements or functions were within ±0.4% of the theoretical values.

4.1.1. General procedures for the preparation of the substituted purine O,N-acetals

A suspension of **25** or **26** and the corresponding purine base in anhydrous acetonitrile (5 mL/mmol) was prepared under argon atmosphere and cooled to 0 °C. At this temperature, TMSCl, HMDS and a 1.0 M solution of $SnCl_4$ in CH_2Cl_2 were added subsequently. The temperature was allowed to rise to 10 °C before microwave irradiating at 140 °C or 160 °C for 5 min. The reactions were quenched by cooling (ice/water bath) and by addition of distilled water. The pH was fixed to 7–8 with a saturated $NaHCO_3$ solution and the aqueous phase extracted with CH_2Cl_2 and EtOAc. The combined organic layers were dried (Na_2SO_4), filtered and evaporated. The residues were purified by flash chromatography under

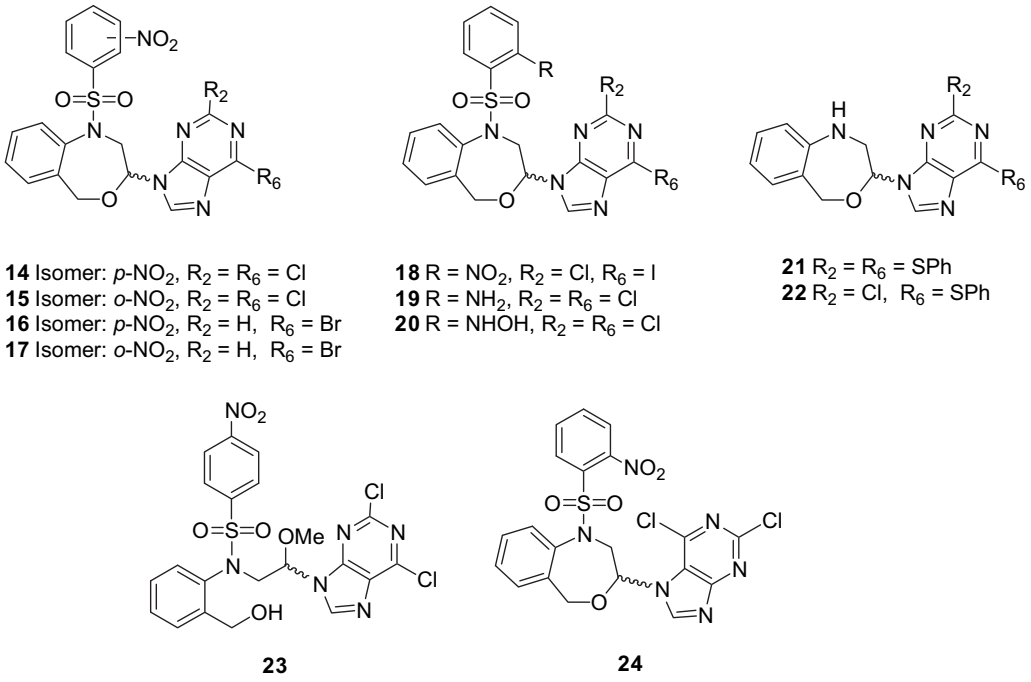

Chart 4.

gradient elution using mixtures of hexane/ethyl acetate (4/1 → 1/1) or CH_2Cl_2/MeOH (100/1 → 100/5) to afford **14**–**17**. Compounds **27** and **28** were also isolated in the reactions. Compound **23** was isolated in the synthesis of **14**. Traces of the *N*-7 regioisomer analogue was detected in the synthesis of **15**.

Three different conditions were investigated; method a): purine (2.5 equiv), TMSCl (4.0 equiv), HMDS (4.0 equiv), $SnCl_4$ (1 M solution in CH_2Cl_2, 4.0 equiv), 160 °C, microwave, 5 min; method b): purine (2.5 equiv), TMSCl (4.0 equiv), HMDS (4.0 equiv), $SnCl_4$ (1 M solution in CH_2Cl_2, 4.0 equiv), 140 °C, microwave, 5 min; method c): purine (1.5 equiv), TMSCl (1.5 equiv), HMDS (1.5 equiv), $SnCl_4$ (1 M solution in CH_2Cl_2, 1.5 equiv), 140 °C, microwave, 5 min.

*4.1.1.1. 1-[(p-Nitrophenyl)sulfonyl]-1,5-dihydro-4,1-benzoxazepin (**27**).* Yellow solid, [method b): 20%], mp: 178–180 °C. ^{1}H NMR ($CDCl_3$, 300 MHz): δ (ppm) 8.33 (d, J = 8.8 Hz, 2H, H-3,5$_{pnitro}$), 7.80 (d, J = 9.1 Hz, 2H, H-2,6$_{pnitro}$), 7.60 (dd, J = 0.9, 7.9 Hz, 1H, H-9), 7.44 (dt, J = 1.5, 7.7 × 2 Hz, 1H, H-8), 7.31 (dt, J = 1.5, 7.5 × 2 Hz, 1H, H-7), 7.14 (dd, J = 1.6, 7.5 Hz, 1H, H-6), 5.94 (d, J = 5.9 Hz, 1H, H-3), 5.78 (d, J = 5.9 Hz, 1H, H-2), 4.01 (s, 2H, H-5). ^{13}C NMR ($CDCl_3$, 75 MHz): δ (ppm) 150.49 (C-4$_{pnitro}$), 142.93 (C-1$_{pnitro}$), 141.37 (C-9a), 138.91 (C-3), 132.26 (C-5a), 130.16, 130.08, 130.00, 128.99 (C-6, 7, 8, 9), 128.90 (C-2$_{pnitro}$ and C-6$_{pnitro}$), 124.55 (C-3$_{pnitro}$ and C-5$_{pnitro}$), 104.27 (C-2), 70.24 (C-5). HR LSIMS (m/z) calcd. for $C_{15}H_{12}N_2O_5NaS$ $(M + Na)^+$ 355.0365, found 355.0364. Anal. $C_{15}H_{12}N_2O_5S$ (C, H, N, S).

*4.1.1.2. 1-[(o-Nitrophenyl)sulfonyl]-1,5-dihydro-4,1-benzoxazepin (**28**).* Brown sirup [method a): 36%; method b): 39%; method c): 29%], ^{1}H NMR ($CDCl_3$, 300 MHz): δ (ppm) 7.87 (dd, J = 1.8, 7.9 Hz, 1H, H-3$_{onitro}$), 7.75–7.63 (m, 2H, H-4$_{onitro}$ and H-5$_{onitro}$), 7.59 (dd, J = 1.3, 7.9 Hz, 1H, H-6$_{onitro}$), 7.47 (dd, J = 1.3, 7.9 Hz, 1H, H-6), 7.40 (ddd, J = 1.8, 7.70 × 2 Hz, 1H, H-7), 7.34 (ddd, J = 1.5, 7.4 × 2 Hz, 1H, H-8), 7.23 (dd, J = 1.5, 7.3 Hz, 1H, H-9), 5.96 (d, J = 5.7 Hz, 1H, H-3), 5.77 (d, J = 5.7 Hz, 1H, H-2), 4.49 (s, 2H, H-5). ^{13}C NMR ($CDCl_3$, 75 MHz): δ (ppm) 148.15, 141.88, 138.77, 134.12, 132.40, 131.57, 131.30, 130.74, 129.65 (×2), 128.97, 128.58, 123.83, 104.05, 70.06 (C-5). HR LSIMS (m/z) calcd. for $C_{15}H_{12}N_2O_5NaS$ $(M + Na)^+$ 355.0365, found 355.0365. Anal. $C_{15}H_{12}N_2O_5S$ (C, H, N, S).

*4.1.1.3. (RS)-2,6-Dichloro-9-[1-(p-nitrobenzenesulfonyl)-1,2,3,5-tetrahydro-4,1-benzoxazepin-3-yl]-9H-purine (**14**).* Yellowish solid [method b): 20%], mp: 173–175 °C. ^{1}H NMR ($CDCl_3$, 300 MHz): δ (ppm) 8.44 (d, J = 8.8 Hz, 2H), 8.17–8.11 (m, 3H), 7.43–7.31 (m, 4H), 6.00 (d, J = 8.8 Hz, 1H), 4.78 (d, J = 13.8 Hz, 1H), 4.74 (dd, J = 1.2, 14.7 Hz, 1H), 4.60 (d, J = 13.8 Hz, 1H), 3.65 (dd, J = 10.0, 14.7 Hz, 1H). ^{13}C NMR ($CDCl_3$, 75 MHz): δ (ppm) 153.72, 152.59, 152.16, 150.79, 146.29, 143.41, 138.78, 136.64, 131.01, 130.52, 130.40, 129.54, 129.10 (×2), 129.05, 125.18 (×2), 84.78, 72.05, 54.56. HR LSIMS (m/z) calcd. for $C_{20}H_{14}N_6O_5NaSCl_2$ $(M + Na)^+$ 543.0021, found 543.0024. Anal. $C_{20}H_{14}Cl_2N_6O_5S$ (C, H, N, S).

*4.1.1.4. (RS)-9-{2-[N-(2-Hydroxymethylphenyl)-p-nitrobenzenesulfonamide]-1-metoxyethyl}-2,6-dichloro-9H-purine (**23**).* White solid [method b): 12%]: mp: 172–174 °C. [conformer A (58%), conformer B (42%)] ^{1}H NMR ($CDCl_3$, 300 MHz): δ (ppm) 8.36–8.28 (m, 5H), 8.12 (s, 1H), 7.80 (d, J = 9.2 Hz, 2H), 7.72 (d, J = 8.8 Hz, 2H), 7.63 (d, J = 7.7 Hz, 1H), 7.61 (d, J = 7.7 Hz, 1H), 7.44–7.39 (m, 2H), 7.30–7.25 (m, 2H), 7.18–7.08 (m, 2H), 6.42 (dd, J = 0.9, 7.9 Hz, 1H), 6.38 (d, J = 0.9, 7.9 Hz, 1H), 5.86 (pt, J = 6.1 Hz, 1H), 5.69 (dd, J = 4.8, 7.5 Hz, 1H), 4.58–4.53 (m, 3H), 4.44–4.36 (m, 2H), 4.27 (d, J = 12.7 Hz, 1H), 4.19 (dd, J = 7.5, 14.5 Hz, 1H), 3.96 (dd, J = 5.7, 14.5 Hz, 1H), 3.30 (s, 6H). ^{13}C NMR ($CDCl_3$, 75 MHz): δ (ppm) 152.9, 150.1, 143.5, 143.3, 141.8, 141.7, 141.1, 136.5, 135.2, 131.3, 130.8, 129.7, 129.4, 129.1, 128.8, 128.6, 128.2, 126.6, 126.4, 123.9, 85.5, 85.2, 60.2, 60.0, 57.0, 56.7, 54.7, 53.6. HR LSIMS (m/z) calcd. for $C_{21}H_{18}N_6O_6NaSCl_2$ $(M + Na)^+$ 575.0283, found 575.0287. Anal. $C_{21}H_{18}Cl_2N_6O_6S$ (C, H, N, S).

*4.1.1.5. (RS)-2,6-Dichloro-9-[1-(o-nitrobenzenesulfonyl)-1,2,3,5-tetrahydro-4,1-benzoxazepin-3-yl]-9H-purine (**15**).* White solid [method a): 32%, b): 37%, c): 47%], mp: 154–155 °C. ^{1}H NMR ($CDCl_3$, 300 MHz): δ (ppm) 8.18 (s, 1H), 8.07 (dd, J = 1.8, 7.9 Hz, 1H), 7.80 (m, 3H), 7.40 (m, 2H), 7.31 (m, 1H), 7.08 (d, J = 7.5 Hz, 1H), 6.09 (dd,

J = 1.8, 10.1 Hz, 1H), 5.05 (d, J = 13.6 Hz, 1H), 4.82 (d, J = 13.6 Hz, 1H), 4.72 (dd, J = 1.8, 13.2 Hz, 1H), 3.84 (dd, J = 10.1, 13.2 Hz, 1H). ^{13}C NMR ($CDCl_3$, 75 MHz): δ (ppm) 153.68, 152.48, 152.38, 148.03, 143.70, 138.89, 137.75, 134.95, 133.71, 132.60, 132.55, 131.03, 130.56, 130.04, 129.58, 128.82, 125.02, 85.22, 72.12, 54.80. HR LSIMS (m/z) calcd. for $C_{20}H_{14}N_6O_5NaSCl_2$ $(M + Na)^+$ 543.0021, found 543.0020. Anal. $C_{20}H_{14}Cl_2N_6O_5S$ (C, H, N, S).

*4.1.1.6. (RS)-2,6-Dichloro-7-[1-(o-nitrobenzenesulfonyl)-1,2,3,5-tetrahydro-4,1-benzoxazepin-3-yl]-7H-purine (**24**).* White solid, [method a): 2%; method b): 1%; method c): 2%], mp: 172–174 °C. ^{1}H NMR (acetone-d_6, 400 MHz): δ (ppm) 8.93 (s, 1H), 8.10–8.07 (m, 3H), 7.94 (m, 1H), 7.57 (d, J = 7.5 Hz, 1H), 7.42–7.44 (m, 2H), 7.21 (d, J = 7.8 Hz, 1H), 6.56 (dd, J = 2.0, 10.2 Hz, 1H), 5.01–4.98 (m, 3H), 4.16 (dd, J = 10.0, 13.7 Hz, 1H). ^{13}C NMR (DMSO-d_6, 100 MHz): δ (ppm) 163.88, 160.85, 152.18, 144.00, 139.25, 137.93, 136.29, 133.91, 132.67, 131.00, 130.89, 130.32, 129.96, 129.54, 128.63, 125.86, 121.01, 85.38, 70.40, 53.85. HR LSIMS (m/z) calcd. for $C_{20}H_{14}Cl_2N_6NaO_5S$ $(M + Na)^+$ 543.0021, found 543.0018. Anal. $C_{20}H_{14}Cl_2N_6O_5S$ (C, H, N, S).

*4.1.1.7. (RS)-6-Bromo-9-[1-(p-nitrobenzenesulfonyl)-1,2,3,5-tetrahydro-4,1-benzoxazepin-3-yl]-9H-purine (**16**).* Viscous oil [method d): 4%]. ^{1}H NMR ($CDCl_3$, 300 MHz): δ (ppm) 8.79 (s, 1H), 8.41 (d, J = 8.8 Hz, 2H), 8.21 (s, 1H), 8.07 (d, J = 8.8 Hz, 2H), 7.42–7.35 (m, 3H), 7.29–7.27 (m, 1H), 6.14(dd, J = 1.8, 10.0 Hz, 1H), 4.80–4.76 (m, 2H), 4.60 (d, J = 13.8 Hz, 1H), 3.75 (dd, J = 10.0, 14.7 Hz, 1H). ^{13}C NMR ($CDCl_3$, 75 MHz): δ (ppm) 152.74, 151.92, 150.73, 146.47, 142.94, 142.80, 138.76, 137.05, 131.91, 130.53, 130.36, 129.58, 128.93 (×2), 128.72, 125.06 (×2), 84.98, 71.84, 54.76. HR LSIMS (m/z) calcd. for $C_{20}H_{15}N_6O_5NaSBr$ $(M + Na)^+$ 552.9906, found 552.9906. Anal. $C_{20}H_{15}BrN_6O_5S$ (C, H, N, S).

*4.1.1.8. (RS)-6-Bromo-9-[1-(o-nitrobenzenesulfonyl)-1,2,3,5-tetrahydro-4,1-benzoxazepin-3-yl]-9H-purine (**17**).* Viscous oil, [method d): 4%], ^{1}H NMR (CD_3OD, 400 MHz): δ (ppm) 8.71 (s, 1H), 8.67 (s, 1H), 8.02 (d, J = 8.0 Hz, 1H), 7.91 (m, 2H), 7.81 (m, 1H), 7.47 (d, J = 8.0 Hz, 1H), 7.40 (t, 1H), 7.33 (m, 1H), 7.09 (d, J = 8.0 Hz, 1H), 6.25 (dd, J = 2.0, 10.2 Hz, 1H), 5.02 (d, J = 13.3 Hz, 1H), 4.84 (d, J = 13.3 Hz, 1H), 4.72 (dd, J = 2.0, 14.9 Hz, 1H), 4.12 (dd, J = 10.2, 14.9 Hz, 1H). ^{13}C NMR (CD_3OD, 75 MHz): δ (ppm) 153.33, 151.27, 149.32, 146.06, 143.62, 140.32, 139.60, 136.30, 135.08, 134.26, 133.64, 132.67, 131.25, 130.69, 130.27, 129.60, 126.72, 86.41, 72.41, 55.14. HR LSIMS (m/z) calcd. for $C_{20}H_{15}N_6O_5NaSBr$ $(M + Na)^+$ 552.9906, found 552.9899. Anal. $C_{20}H_{15}BrN_6O_5S$ (C, H, N, S).

*4.1.2. Substitutions on **15**: formation of 6-iodo derivative **18***

To a solution of **15** (1.0 equiv) in butanone (20 mL/mmol), NaI (20.0 equiv) and TFA (5.0 equiv) were added subsequently at −15 °C and the reaction mixture was stirred at this temperature for 6 h. The solvent was evaporated and water was added to the residue. The aqueous layer was extracted (CH_2Cl_2) and the combined organic layers were washed ($NaHSO_4$ and brine), dried (Na_2SO_4) and evaporated. Purification of **18** was carried out by flash chromatography using EtOAc/hexane 1/2 as eluent.

*4.1.2.1. (RS)-2-Chloro-6-iodo-9-[1-(o-nitrobenzenesulfonyl)-1,2,3,5-tetrahydro-4,1-benzoxazepin-3-yl]-9H-purine (**18**).* Yellow solid (66%), mp: 129–132 °C ^{1}H NMR ($CDCl_3$, 300 MHz): δ (ppm) 8.18 (s, 1H), 8.08 (d, J = 8.0 Hz, 1H), 7.81–7.79 (m, 3H), 7.42–7.40 (m, 2H), 7.31–7.32 (m, 1H), 7.10 (d, J = 8.0 Hz, 1H), 6.06 (dd, J = 8.0, 16.0 Hz, 1H), 5.04 (dd, J = 8.0, 12.0 Hz, 1H), 4.82 (d, J = 12.0 Hz, 1H), 4.73 (dd, J = 4.0, 16.0 Hz, 1H), 3.82–3.80 (m, 1H). ^{13}C NMR ($CDCl_3$, 75 MHz): δ (ppm) 153.10, 152.46, 152.34, 148.81, 147.86, 143.64, 138.85, 137.72, 137.68, 134.90, 133.68, 132.57, 132.52, 130.53, 130.00, 128.82, 124.99, 85.18, 72.12, 54.76. HR LSIMS (m/z) calcd. for $C_{20}H_{14}N_6O_5NaSClI$ $(M + Na)^+$ 634.9377, found 634.9381. Anal. $C_{20}H_{14}ClIN_6O_5S$ (C, H, N, S).

*4.1.3. Reduction of **15**: formation of amino **19** and hydroxylamino **20** derivatives*

$SnCl_2 \cdot 2H_2O$ (5.0 equiv) was added at room temperature to a suspension of **15** in EtOH (2.5 mL/mmol) and heated at the reflux temperature for 2 h. The reaction mixture was then cooled at 0 °C and the pH was fixed to 7–8 with saturated $NaHCO_3$ solution. The aqueous layer was extracted with CH_2Cl_2 and the combined organic layers were washed with brine, dried (Na_2SO_4) and evaporated. Purification of **19** and **20** was carried out by flash chromatography using CH_2Cl_2/acetone (9.9/0.1) as eluent.

*4.1.3.1. (RS)-9-[1-(o-Aminobenzenesulfonyl)-1,2,3,5-tetrahydro-4,1-benzoxazepin-3-yl]-2,6-dichloro- 9H-purine (**19**).* White solid (35%); mp: 225–227 °C. ^{1}H NMR ($CDCl_3$, 400 MHz): δ (ppm) 8.14 (s, 1H), 7.83–7.81 (m, 2H), 7.63 (dd, J = 1.6, 8.2 Hz, 1H), 7.55 (dd, J = 1.2, 7.8 Hz, 1H), 7.44–7.25 (m, 4H), 6.02 (dd, J = 2.0, 10.2 Hz, 1H), 4.70–4.67 (m, 3H), 3.53 (dd, J = 10.2, 14.9 Hz, 1H). ^{13}C NMR ($CDCl_3$, 75 MHz): δ (ppm) 153.52, 152.34, 152.15, 145.42, 143.81, 143.49, 139.57, 136.83, 135.45, 130.70, 130.07, 129.99, 129.96, 128.76, 121.59, 118.31, 118.25, 84.37, 71.90, 54.23. HR LSIMS (m/z) calcd. for $C_{20}H_{16}N_6O_3NaSCl_2$ $(M + Na)^+$ 513.0279, found 513.0284. Anal. $C_{20}H_{16}Cl_2N_6O_3S$ (C, H, N, S).

*4.1.3.2. (RS)-2,6-Dichloro-9-[1-(o-hydroxylaminobenzene-sulfonyl)-1,2,3,5-tetrahydro-4,1-benzoxazepin-3-yl]-9H-purine (**20**).* Viscous oil (35%). ^{1}H NMR ($CDCl_3$, 400 MHz): δ (ppm) 8.13 (s, 1H), 7.42 (ddd, J = 1.2, 8.2, 16.6 Hz, 1H), 7.60 (ddd, J = 1.6, 7.4 × 2 Hz, 1H), 7.47 (ddd, J = 1.6, 7.8 Hz, 1H), 7.36 (ddd, J = 1.2, 7.4 Hz, 1H), 7.29 (dd, J = 1.4, 8.0 Hz, 1H), 7.26 (m, 1H), 7.20 (dd, J = 1.6, 7.4 Hz, 1H), 6.84 (ddd, J = 1.2, 7.8 Hz, 1H), 6.66 (dd, J = 2.1, 10.0 Hz, 1H), 4.77 (dd, J = 2.0, 14.9 Hz, 1H), 4.38 (d, J = 13.7 Hz, 1H), 3.67 (d, J = 13.3 Hz, 1H), 3.53 (dd, J = 10.3, 15.1 Hz, 1H). ^{13}C NMR ($CDCl_3$, 75 MHz): δ (ppm) 153.64, 153.24, 151.86, 147.03, 143.82, 138.29, 136.97, 135.41, 131.70, 131.12, 130.15, 129.75, 129.71, 129.20, 123.84, 120.71, 115.20, 83.23, 71.35, 54.70. HR LSIMS (m/z) calcd. for $C_{20}H_{17}Cl_2N_6O_4S$ $(M + H)^+$ 507.0404, found 507.0441. Anal. $C_{20}H_{16}Cl_2N_6O_4S$ (C, H, N, S).

*4.1.4. Substitutions on **15**: formation of 2,6-dithiophenyl **21** and 6-thiophenyl **22** derivatives*

*4.1.4.1. (RS)-2,6-Dithiophenyl-9-[1,2,3,5-tetrahydro-4,1-benzoxazepin-3-yl]-9H-purine (**21**).* K_2CO_3 (3.0 equiv) and PhSH (1.1 equiv) were added at room temperature to a solution of **15** (1.0 equiv) in DMF (5 mL/mmol). The mixture was stirred at room temperature for 4 h. The solvent was evaporated and water was added to the residue. The aqueous layer was extracted with CH_2Cl_2 and the combined organic layers were washed with brine, dried (Na_2SO_4) and evaporated. Purification of **21** was carried out by flash chromatography using EtOAc/hexane 1/4 as eluent. White solid, (42%), mp: 82–86 °C. ^{1}H NMR ($CDCl_3$, 300 MHz): δ (ppm) 8.17 (s, 1H), 7.6 (ddd, J = 0.9, 7.5 × 2 Hz, 1H), 7.53–718 (m, 13H), 6.92 (d, J = 7.9 Hz, 1H), 6.03 (dd, J = 2.4, 7.7 Hz, 1H), 4.95 (d, J = 14.1 Hz, 1H), 4.80 (d, J = 14.1 Hz, 1H), 3.73 (dd, J = 2.6, 13.6 Hz, 1H), 3.59 (dd, J = 7.5, 13.6 Hz, 1H). ^{13}C NMR ($CDCl_3$, 75 MHz): δ (ppm) 177.21, 165.50, 161.25, 149.10, 141.13, 135.39 (×2), 135.26 (×2), 130.25, 129.72 (×2), 129.42, 129.39, 129.26 (×2), 129.06 (×2), 129.00, 128.55, 127.02, 122.21, 119.29, 85.22, 70.48, 51.79, one carbon missing. HR LSIMS (m/z) calcd. for $C_{26}H_{21}N_5ONaS_2$ $(M + Na)^+$ 506.1085, found 506.1084. Anal. $C_{26}H_{21}N_5OS_2$ (C, H, N, S).

*4.1.4.2. (RS)-2-Chloro-6-phenylthio-9-[1,2,3,5-tetrahydro-4,1-benzoxazepin-3-yl]-9H-purine (**22**).* K_2CO_3 (1.6 equiv) and PhSH (0.8 equiv) were added at room temperature to a solution of **15**

(1.0 equiv) in DMF (5 mL/mmol). The mixture was stirred at room temperature for 4 h. The solvent was evaporated and water was added to the residue. The aqueous layer was extracted with CH_2Cl_2 and the combined organic layers were washed with brine, dried (Na_2SO_4) and evaporated. Purification of **22** was carried out by flash chromatography using EtOAc/hexane 1/2 as eluent. White solid, (40%), mp: 161–163 °C. ^{1}H NMR ($CDCl_3$, 300 MHz): δ (ppm) 8.27 (s, 1H), 7.95 (ddd, $J = 0.4$, 7.5 Hz, 1H), 7.64 (m, 2H), 7.46 (m, 3H) 7.19 (m, 2H), 6.87 (d, $J = 7.9$ Hz, 1H), 6.11 (dd, $J = 2.2$, 7.4 Hz, 1H), 4.88 (s, 2H), 3.83 (dd, $J = 2.2$, 13.6 Hz, 1H), 3.40 (dd, $J = 7.4$, 13.6 Hz, 1H). ^{13}C NMR ($CDCl_3$, 75 MHz): δ (ppm) 163.13, 154.06, 149.70, 147.99, 142.22, 135.59 (×2), 129.97, 129.75, 129.73, 129.56, 129.50 (×2), 128.46, 126.71, 122.03, 119.19, 85.02, 71.02, 52.85. HR LSIMS (m/z) calcd. for $C_{20}H_{16}N_5ONaSCl$ $(M + Na)^+$ 432.0662, found 432.0660. Anal. $C_{20}H_{16}ClN_5O_5S$ (C, H, N, S).

*4.1.4.3. Resolution of (RS)-**14**.* (*RS*)-9-[1-(*p*-Nitrobenzenesulfonyl)-1,2,3,5-tetrahydro-4,1-benzoxazepin-3-yl]-2,6-dichloro-9*H*-purine (**14**) is resolved into its enantiomers: the one that elutes first is (*R*)-**14** (retention time = 8.5 min), and the one which comes second is (*S*)-**14** (retention time = 19.8 min), using a column CHIRALPAK® IA (DAICEL CHEMICAL INDUSTRIES, LTD.) semipreparative, and as eluent a mixture of hexane/*t*-BuOMe/*i*PrOH (26/65/9).

4.2. Biology

4.2.1. Cell culture

MCF-7 and MDA-MB-231 cells were grown at 37 °C in an atmosphere containing 5% CO_2, with Dubelcco's modified Eagle Medium (DMEM) (Gibco, Grand Island, NY) supplemented with 10% heat-inactivated fetal bovine serum (FBS) (Gibco), 2% L-glutamine, 2.7% sodium bicarbonate, 1% Hepes buffer, 40 mg/L gentamicin and 500 mg/L ampicillin.

4.2.2. Drugs and drug treatments

The drugs were dissolved in DMSO or water and stored at −20 °C. For each experiment, the stock solutions were further diluted in medium to obtain the desired concentrations. The final solvent concentration in cell culture was ≤0.1% v/v of DMSO, a concentration without effect on cell replication. Parallel cultures of cells in medium with DMSO were used as controls.

4.2.3. Cytotoxicity assays in vitro

The effect of anticancer drugs on cell viability was assessed using the sulforhodamine-B colorimetric assay [38]. Aliquots of MCF-7 cells suspension (1×10^3 cells/well) were seeded onto 24-well plates and incubated for 24 h. The cells were then treated with different concentrations of drugs in the culture medium. Three days later, the wells were aspirated, fresh medium and treatment were added, and cells were maintained for 3 additional days. Thereafter, cells were processed as described previously [38], using a Titertek Multiscan apparatus (Flow, Irvine, California) at 492 nm. We evaluated linearity of the SRB assay with cell number for each cell line before each cell growth experiment. The IC_{50} values were calculated from semilogarithmic dose–response curves by linear interpolation. All of the experiments were plated in triplicate wells and were carried out at least twice.

4.2.4. Cell-cycle distribution analysis

The cells at 70% confluence were treated with either DMSO alone or with concentrations of the compounds determined by their IC_{50} values. FACS analysis was performed after 48 h of treatment as described [38]. All experiments were performed in triplicate and yielded similar results.

4.2.5. Apoptosis detection by staining with annexin V-FITC and propidium iodide

The annexin V-FITC apoptosis detection kit I (Pharmingen, San Diego, CA, USA) was used to detect apoptosis by flow cytometry according to Marchal et al. [38]. All experiments were performed in triplicate and yielded similar results.

4.2.6. Apoptosis detection by confocal microscopy

Cells (5×10^3 cells/well) were seeded onto Labtek chamber-slide 8-well plates. Cells were allowed to adhere for 24 h before dosing with required concentrations of compounds. Culture medium was removed and cells were washed with cold 1X PBS. After that, cells were incubated with both Annexin V-FITC and propidium iodide for 15 min at room temperature in the dark. Cells were then washed with binding buffer, prepared with mounting medium and cover slips before confocal microscopic imaging [42]. Cells were imaged by confocal microscopy using a Leica SP2 Confocal Microscope.

4.2.7. Toxicity assays in vivo

Acute toxicity was determined in six-week old BALB/c female mice (average, 20 g weight) during 2 weeks. (*RS*)-**14** dissolved in 0.25 mL of a mixture of 0.9% sodium chloride and DMSO was administered in BALB/c in a single i.p. bolus injection ($n = 25$) at dose levels of 50, 75, 100, 150 and 200 mg/kg or *via* gavage ($n = 25$) in a single p.o. bolus at dose levels of 0.05, 0.5, 5 and 50 mg/kg. Control mice were inoculated with the same volume of sodium chloride (control group) and DMSO alone (DMSO group). Mice were maintained under standard conditions and for each treatment schedule, were weighed and assessed twice weekly for systemic toxicity (listlessness, weight loss) and local toxicity (alopecia, skin reaction, and leg motility).

Acknowledgments

This study was supported by the European Commission (A.C-G. Marie Curie Programme MERG-CT-2005-030616) and the Instituto de Salud Carlos III (Fondo de Investigación Sanitaria) through projects no. PI070227 and PI070527. The project "Factoría de Cristalización, CONSOLIDER INGENIO-2010" (CSD2006-00015) provided X-ray structural facilities for this work. We gratefully acknowledge the BM16 Spanish beamline at ESRF (Grenoble, France) for access to synchrotron radiation and for helpful assistance during data collection. D Ch-L thanks CSD2006-00015 for his research contract.

Appendix. Supplementary data

Supplementary data associated with this article can be found, in the online version, at doi:10.1016/j.ejmech.2010.11.011.

References

[1] B.W. Stewart, P. Kleihues (Eds.), World Cancer Report, International Agency for Research on Cancer, World Health Organization, 2003.
[2] P. Fresco, F. Borges, M.P.M. Marques, C. Diniz, The anticancer properties of dietary polyphenols and its relation with apoptosis, Curr. Pharm. Des. 16 (2010) 114–134.
[3] M. Hajduch, L. Havlieek, J. Vesely, R. Novotny, V. Mihal, M. Strnad, Synthetic cyclin-dependent kinase inhibitors: new generation of potent anti-cancer drugs, Adv. Exp. Med. Biol. 457 (1999) 341–353.
[4] C.J. Sherr, Cancer cell cycles, Science 274 (1996) 1672–1677.
[5] S. Nagata, Apoptosis by death factor, Cell 88 (1997) 355–365.
[6] U. Testa, Apoptotic mechanisms in the control of erythropoiesis, Leukemia 18 (2004) 1176–1199.
[7] J. Zivny, P. Klener Jr., R. Pytlik, L. Andera, The role of apoptosis in cancer development and treatment: focusing on the development and treatment of hematologic malignancies, Curr. Pharm. Des. 16 (2010) 11–33.
[8] E. Saniger, J.M. Campos, A. Entrena, J.A. Marchal, I. Suárez, A. Aránega, D. Choquesillo, J. Niclós, M.A. Gallo, A. Espinosa, Medium benzene-fused oxacycles

with the 5-fluorouracil moiety: synthesis. Antiproliferative activities and apoptosis induction in breast cancer cells, Tetrahedron 59 (2003) 5457–5467.
[9] E. Saniger, J.M. Campos, A. Entrena, J.A. Marchal, H. Boulaiz, A. Aránega, M.A. Gallo, A. Espinosa, Neighbouring-group participation as the key step in the reactivity of acyclic and cyclic salicyl-derived *O,O*-acetals with 5-fluorouracil. Antiproliferative activity, cell cycle dysregulation and apoptotic induction of new *O,N*-acetals against breast cancer cells, Tetrahedron 59 (2003) 8017–8026.
[10] J.A. Marchal, M.C. Núñez, I. Suárez, M. Díaz-Gavilán, J.A. Gómez-Vidal, H. Boulaiz, F. Rodríguez-Serrano, A. Aránega, M.A. Gallo, A. Espinosa, J.M. Campos, A synthetic uracil derivative with antitumor activity through decreasing cyclin D1 and Cdk1, and increasing p21 and p27 in MCF-7 cells, Breast Cancer Res. Tr. 105 (2007) 237–246.
[11] M.C. Núñez, A. Entrena, F. Rodríguez-Serrano, J.A. Marchal, A. Aránega, M.A. Gallo, A. Espinosa, J.M. Campos, Synthesis of novel 1-(2.3-dihydro-5*H*-4.1-benzoxathiepin-3-yl)-uracil and -thymine, and their corresponding *S*-oxidized derivatives, Tetrahedron 61 (2005) 10363–10369.
[12] M. Díaz-Gavilán, J.A. Gómez-Vidal, A. Entrena, M.A. Gallo, A. Espinosa, J.M. Campos, Study of the factors that control the ratio of the products between 5-fluorouracil, uracil, and tetrahydrobenzoxazepine *O,O*-acetals bearing electron-withdrawing groups on the nitrogen atom, J. Org. Chem. 71 (2006) 1043–1054.
[13] M. Díaz-Gavilán, J.A. Gómez-Vidal, F. Rodríguez-Serrano, J.A. Marchal, O. Caba, A. Aránega, M.A. Gallo, A. Espinosa, J.M. Campos, Anticancer activity of (1.2.3.5-tetrahydro-4.1-benzoxazepine-3-yl)-pyrimidines and -purines against the MCF-7 cell line: preliminary cDNA microarray studies, Bioorg. Med. Chem. Lett. 18 (2008) 1457–1460.
[14] M.C. Núñez, M. Díaz-Gavilán, A. Conejo-García, O. Cruz-López, M.A. Gallo, A. Espinosa, J.M. Campos, Design, synthesis and anticancer activity against the MCF-7 cell line of benzo-fused 1.4-dihetero seven- and six-membered tethered pyrimidines and purines, Curr. Med. Chem. 15 (2008) 2614–2631.
[15] C.O. Kappe, Synthetic methods. Controlled microwave heating in modern organic synthesis, Angew. Chem. Int. Ed. 43 (2004) 6250–6284.
[16] B.L. Hayes, Recent advances in microwave-assisted synthesis, Aldrichim. Acta 37 (2004) 66–77.
[17] A. De la Hoz, A. Díaz-Ortiz, A. Moreno, Microwaves in organic synthesis. Thermal and non-thermal microwave effects, Chem. Soc. Rev. 34 (2005) 164–178.
[18] C.O. Kappe, A. Stadler, Microwaves in Organic and Medicinal Chemistry. Wiley-VCH, Weinheim, 2005.
[19] P. Lidström, J.P. Tierney (Eds.), Microwave-assisted Organic Synthesis, Blackwell, Oxford, 2005.
[20] A. Loupy, Microwaves in Organic Synthesis. Wiley-VCH, Weinheim, 2002.
[21] B.L. Hayes, Microwave Synthesis: Chemistry at the Speed of Light. CEM, Matthews, NC, 2002.
[22] F. Al-Obeidi, R.E. Austin, J.F. Okonya, D.R.S. Bond, Microwave-assisted solid-phase synthesis (MASS): parallel and combinatorial chemical library synthesis, Mini-Rev. Med. Chem. 3 (2003) 449–460.
[23] C. Kappe, O.D. Dallinger, The impact of microwave synthesis on drug discovery, Nat. Rev. Drug Discov. 5 (2006) 51–63.
[24] A. Conejo-García, M.C. Núñez, J.A. Marchal, F. Rodríguez-Serrano, A. Aránega, M.A. Gallo, A. Espinosa, J.M. Campos, Regioespecific microwave-assisted synthesis and cytotoxic activity against human breast cancer cells of (RS)-6-substituted-7- or 9-(2.3-dihydro-5H-1.4-benzodioxepin-3-yl)-7H- or -9H-purines, Eur. J. Med. Chem. 43 (2008) 1742–1748.
[25] M. Díaz-Gavilán, F. Rodríguez-Serrano, J.A. Gómez-Vidal, J.A. Marchal, A. Aránega, M.A. Gallo, A. Espinosa, J.M. Campos, Synthesis of tetrahydrobenzoxazepine acetals with electron-withdrawing groups on the nitrogen atom. Novel scaffolds endowed with anticancer activity against breast cancer cells, Tetrahedron 60 (2004) 11547–11557.
[26] M. Díaz-Gavilán, D. Choquesillo-Lazarte, J.M. González-Pérez, M.A. Gallo, A. Espinosa, J.M. Campos, Synthesis and reactivity of (*RS*)-6-chloro-7- or 9-(1,2,3,5-tetrahydro-4,1-benzoxazepin-3-yl)-7*H*- or 9*H*-purines bearing a nitrobenzenesulfonyl group on the nitrogen atom, Tetrahedron 63 (2007) 5274–5286.
[27] M.C. Núñez, M.E. García-Rubiño, A. Conejo-García, O. Cruz-López, M. Kimatrai, M.A. Gallo, A. Espinosa, J.M. Campos, Homochiral drugs: a demanding tendency of the pharmaceutical industry, Curr. Med. Chem. 16 (2009) 2064–2074.
[28] J.A. Marchal, A. Aránega, A. Conejo García, M.A. García Chaves, O. Cruz-López, H. Boulaiz, F. Rodríguez-Serrano, C. Cativiela, M. Perán, A.I. Jiménez, J.M. García-Ruiz, D. Choquesillo-Lasarte, J.M. Campos, Enantiómeros de derivados benzoheteroepínicos y su uso como agentes anticancerígenos. Universidad de Granada, 2010, P201030415.
[29] M.C. Núñez, F. Rodríguez-Serrano, J.A. Marchal, O. Caba, A. Aránega, M.A. Gallo, A. Espinosa, J.M. Campos, 6′-Chloro-7- or 9-(2,3-dihydro-5*H*-4,1-benzoxathiepin-3-yl)-7*H*- or 9*H*-purines and their corresponding sulfones as a new family of cytotoxic drugs, Tetrahedron 63 (2007) 183–190.
[30] H. Liu, L. Xu, M. Zhao, W. Liu, C. Zhang, S. Zhou, Enantiomer-specific, bifenthrin-induced apoptosis mediated by MAPK signalling pathway in Hep G2 cells, Toxicology 261 (2009) 119–125.
[31] M.D. Shelley, L. Hartley, R.G. Fish, P. Groundwater, J.J.G. Morgan, D. Mort, M. Mason, A. Evans, Stereo-specific cytotoxic effects of gossypol enantiomers and gossypolone in tumour cell lines, Cancer Lett. 135 (1999) 171–180.
[32] J.C. Lai, B.D. Brown, A.M. Voskresenskiy, S. Vonhoff, S. Klussman, W. Tan, M. Colombini, R. Weeratna, P. Miller, L. Benimetskaya, C.A. Stein, Comparison of D-G3139 and its enantiomer L-G3139 in melanoma cells demonstrates minimal in vitro but dramatic in vivo chiral dependency, Mol. Ther. 15 (2007) 270–278.
[33] N.M. Brown, C.A. Belles, S.L. Lindley, L.D. Zimmer-Nechemias, X. Zhao, D.P. Witte, M.O. Kim, K.D.R. Setchell, The chemopreventive action of equol enantiomers in a chemically induced animal model of breast cancer, Carcinogenesis 31 (2010) 886–893.
[34] J.L. Grem, D. Nguyen, B.P. Monahan, V. Kao, F.J. Geoffroy, Sequence-dependent antagonism between fluorouracil and paclitaxel in human breast cancer cells, Biochem. Pharmacol. 58 (1999) 477–486.
[35] K.J. Duncan, K.A. Eckert, G.A. Clawson, Mechanisms of growth inhibition in human papillomavirus positive and negative cervical cancer cells by the chloromethyl ketone protease inhibitor, succinyl-alanine-alanine-proline-phenylalanine chloromethyl ketone, J. Pharmacol. Exp. Ther. 330 (2009) 359–366.
[36] D.E. Saunders, W.D. Lawrence, C. Christensen, N.L. Wappler, H. Ruan, G. Deppe, Paclitaxel-induced apoptosis in MCF-7 breast cancer cells, Int. J. Cancer 70 (1997) 214–220.
[37] A. Chadderton, D.J. Villeneuve, S. Gluck, A.F. Kirwan-Rhude, B.R. Gannon, D.E. Blais, A.M. Parissenti, Role of specific apoptotic pathways in the restoration of paclitaxel-induced apoptosis by valspodar in doxorubicin-resistant MCF-7 breast cancer cells, Breast Cancer Res. Tr. 59 (2000) 231–244.
[38] J.A. Marchal, H. Boulaiz, I. Suárez, E. Saniger, J. Campos, E. Carrillo, J. Prados, M.A. Gallo, A. Espinosa, A. Aránega, Growth inhibition, G_1-arrest, and apoptosis in MCF-7 human breast cancer cells by novel highly lipophilic 5-fluorouracil derivatives, Invest. New Drugs 22 (2004) 379–389.
[39] A.S. Lundberg, R.A. Weinberg, Control of the cell cycle and apoptosis, Eur. J. Cancer 35 (1999) 531–539.
[40] A. De Fátima, W.F. Zambuzzi, L.V. Modolo, C.A.B. Tarsitano, F.R. Gadelha, S. Hyslop, J.E. de Carvalho, I. Salgado, C.V. Ferreira, R.A. Pilli, Cytotoxicity of goniothalamin enantiomers in renal cancer cells: involvement of nitric oxide, apoptosis and autophagy, Chem. Biol. Interact. 176 (2008) 143–150.
[41] L. Formigli, S. Zecchi Orlandini, S. Capaccioli, M.F. Poupon, D. Bani, Energy-dependent types of cell death in MCF-7 breast cancer cell tumors implanted into nude mice, Cells Tissues Organs 170 (2002) 99–110.
[42] J.L. Gooch, D. Yee, Strain-specific differences in formation of apoptotic DNA ladders in MCF-7 breast cancer cells, Cancer Lett. 144 (1999) 31–37.